CrystEngComm

Synthesis and functionalization of phase-pure NU-901 for enhanced CO_2 adsorption: The influence of zirconium salt and modulator on topology and phase purity

Journal:	*CrystEngComm*
Manuscript ID	CE-COM-08-2018-001454.R1
Article Type:	Communication
Date Submitted by the Author:	25-Sep-2018
Complete List of Authors:	Garibay, Sergio; Edgewood Chemical Biological Center, Iordanov, Ivan; Edgewood Chemical Biological Center Islamoglu, Timur; Northwestern University, Department of Chemistry DeCoste, Jared; jared.b.decoste2.ctr@mail.mil, Aberdeen Proving Ground Farha, Omar; Northwestern University, Department of Chemistry

CrystEngComm

COMMUNICATION

Received 00th January 20xx,
Accepted 00th January 20xx

DOI: 10.1039/x0xx00000x
www.rsc.org/

Synthesis and functionalization of phase-pure NU-901 for enhanced CO_2 adsorption: The influence of zirconium salt and modulator on topology and phase purity

S. J. Garibay,[a] I. Iordanov,[a] T. Islamoglu,[b] J. B. DeCoste,*[a] and O. K. Farha*[b,c]

The synthesis of NU-901, a microporous Zr_6-based MOF with scu topology, often contains NU-1000 csq phase impurities. This work demonstrates that the use of certain Zr-salts and carboxylic acid modulators affect the formation of phase impurities. Phase-pure NU-901 was solvothermally synthesized and functionalized with amines through the use of solvent-assisted linker incorporation (SALI) resulting in more than double the typical CO_2 adsorption capacity of NU-901.

Introduction

Metal-organic frameworks (MOFs) are hybrid porous materials composed of inorganic secondary-building units (SBUs) (metal ions or metal oxide clusters) and bridging organic multitopic linkers.[1] The modular synthetic feasibility of utilizing various inorganic and organic building blocks, i.e. reticular chemistry,[2] give rise to a multitude of diverse network topologies. Their tunable pore compositions have enabled their use in a wide range of applications such as gas storage or separations,[3] and catalysis,[4] which require high surface areas, ultra-micropores, and facile substrate diffusion, respectively. However, many MOFs prove to be hydrolytically unstable for most practical applications.[5]

Zr-based MOFs provide robust chemical stabilities due to their strong metal-carboxylate coordination bonds, which enable their use in realistic and often under harsh catalytic conditions.[6] Recently, Zr MOFs have been reported as chemically stable heterogeneous catalysts.[7, 8] Tetratopic carboxylate linkers and Zr_6 cubo-octahedral SBU can generate multiple network topologies such as **csq**,[9, 10] **scu**,[11, 12] **shp**,[13] **ftw**,[10, 14, 15] **she**,[16] and **sqc**[17] under different synthetic conditions. However, these solvothermal synthetic conditions often generate partial phase impurities containing distinct network topologies.[18] Given that topology often affects the inclusion and diffusion of the substrate into the pores of a MOF, these phase impurities may significantly alter performance in gas separation and catalytic applications.[19]

Recent computational and synthetic efforts have been spent understanding the role of linkers in the structural design and formation of Zr-based MOFs with distinct topologies.[20] For example, Matzger,[21] and Zhou[22] et al. studied the geometric influence of tetratopic organic linkers on the resulting network topologies with Zr_6 clusters. They found that the linker's flexibility, due to shape or substituent steric hindrance, dictate formation of specific topologies. While the influence of linker torsion angles and geometries on topology have been extensively utilized and observed within MOF synthesis,[23-25] it is the variable connectivity of the Zr_6 SBU to the linker that complicates predicting topology through reticular chemistry. The Zr_6 SBU is commonly 12 connected, but can be 10, 8, 6 or 4 connected.[26, 27] So while linker flexibility may help drive selective topology formation, it necessitates costly multi-step organic synthesis and does not factor-in the prominent role of the SBU in directing MOF formation nor the modulators used in their synthesis.

The use of modulators, i.e. mono carboxylic acids, during solvothermal synthesis has been proven to significantly affect MOF formation and alter their physical properties.[28] The concentration of modulator not only regulates the particle size of the MOF,[29] but may induce missing-linker or missing-node defects.[30] Depending on the type of modulator used, the degree of defect sites significantly enhances surface area and catalytic properties of Zr-based MOFs.[19, 31, 32] Modulators not only affect the MOF's size and amount of missing-linkers, it can influence the topology of the framework.[33-35] Farha and coworkers[36] along with Penn and coworkers[37] obtained phase-pure NU-1000 by suppressing the formation of a polymorph NU-901-like impurity through the use of trifluoroacetic acid or 4-phenylbenzoic acid modulators (Fig. 1). While NU-1000 has been extensively used for inclusion of catalytically active species through solvent-assisted linker incorporation (SALI),[38] solvothermal- or atomic layer-deposition in MOFs (SIM or AIM),[39, 40] it has been rarely used for gas-separation applications due its inherent large percentage of mesoporosity that reduces the adsorption strength of the analyte with the internal pore surface.

---

[a] Edgewood Chemical Biological Center, US Army Research, Development, and Engineering Command, 5183 Blackhawk Road, Aberdeen Proving Ground, Maryland 21010, USA.
[b] Department of Chemistry the International Institute of Nanotechnology, Northwestern University, 2145 Sheridan Road, Evanston, Illinois 60208, USA
[c] Department of Chemistry, Faculty of Science, King Abdulaziz University, Jeddah 21589, Saudi Arabia

† Electronic Supplementary Information (ESI) available. See DOI: 10.1039/x0xx00000x

Herein, we describe the solvothermal synthesis of phase-pure NU-901 through the use of 4-aminobenzoic acid modulator and $Zr(acac)_4$ salt. NU-901, is comprised of eight-connected $Zr_6(\mu_3\text{-}OH)_4(\mu_3O)_4(OH)_4(OH_2)_4$ SBU nodes and 1,3,6,8-tetrakis-(*p*-benzoate)-pyrene (H_4TBAPy) linkers which form microporous diamond-shaped channels with **scu** topology. The use of SALI allows the facile incorporation of amines within the micropores of NU-901. The functionalized MOFs designated NU-901-SALI-BA-X, (BA = benzoic acid, X = functional group) provides an ideal pore environment for enhanced CO_2 adsorption.

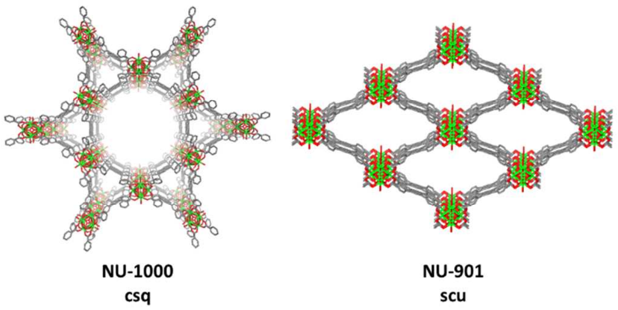

Fig 1. The micro/mesoporous NU-1000 with **csq** network topology (left), and the microporous NU-901 with **scu** network topology (right).

Results and discussion

NU-1000 is typically solvothermally synthesized by adding the H_4TBAPy linker to a DMF solution of *in-situ* pre-formed Zr_6 SBUs with benzoic acid modulators. The resulting framework consists of an 8-connected Zr_6 SBU with mesoporous hexagonal channels and **csq** topology. NU-901, similarly contains 8-connected Zr_6 SBUs, however, it has microporous diamond channels with **scu** topology. Until recently the only reported synthesis of NU-901 was achieved by growing the MOF on a fluorine-doped tin oxide (FTO) glass substrate.[41] While this method generated pure-phase NU-901 in low yields, its phase purity diminishes when bulk large scale synthesis is attempted under analogous reaction conditions. Applications such as CO_2 capture requires industrial scale MOF synthesis. In order to mitigate costs we explored cheaper alternative coupling catalyst for ligand synthesis. The use of 10 mol% catalyst loading of $NiCl_2(PPh_3)_2$/ PPh_3 resulted in comparable yields (59%) of $TBAPyOEt_4$ to that of the costly $Pd(PPh_3)_4$ (see synthetic conditions in the ESI†).

Zr-based MOFs have been typically synthesized with either $ZrCl_4$ or $ZrOCl_2$ salts, however, these precursors generate halogenated waste which is seen as a detriment for green synthesis. Moreover, while extensive work has been spent on understanding the role of modulators in the synthesis of Zr-based MOFs, the effect of zirconium salts has rarely been given attention. We sought to investigate the effects of non-halogenated zirconium salts in the formation of NU-1000 or NU-901. Under standardized reaction conditions with benzoic acid, $ZrO(NO_3)_2$ gives NU-1000 while $Zr(acac)_4$ gives a mixture of NU-1000 and NU-901 as evidenced by PXRD (Fig. 2). The use of $Zr(acac)_4$ appears to inhibit NU-1000 formation as evidenced by the diminished PXRD peak (2Θ = 2.5°) characteristic of the (100) plane. Moreover, phase impurities are apparent by the characteristic mesoporous steps at $p/p_o = 0.25$ in the nitrogen adsorption isotherms (Fig. 3). The phase heterogeneity of the MOF generated by $Zr(acac)_4$ and benzoic acid can be readily observed by SEM imaging (Fig S17 in the ESI†).

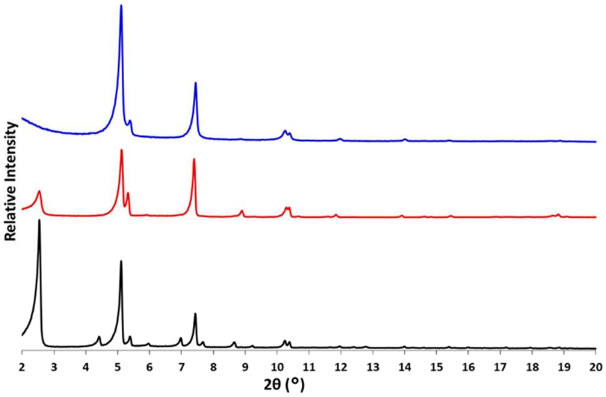

Fig 2. PXRD patterns of HCl-activated MOFs prepared with $ZrO(NO_3)_2$ + BA; NU-1000 (bottom), $Zr(acac)_4$ + BA; NU-1000/NU-901 (middle), and $Zr(acac)_4$ + 4-NH_2-BA; NU-901 (top). BA = benzoic acid

Recently, several reports have attempted the synthesis of NU-901 in bulk through the use of halogenated Zr salts and 4-aminobenzoic acid or benzoic acid modulators, however, phase impurities are still apparent in the nitrogen adsorption isotherms.[42, 43] Given the ability of 4-aminobenzoic acid and $Zr(acac)_4$ of nearly inhibiting NU-1000 formation, we hypothesized that their combination would induce phase-pure NU-901. Under analogous reactions conditions mentioned above, the use of $Zr(acac)_4$ and 4-aminobenzoic acid indeed generated phase-pure NU-901 with **scu** topology. No detectable traces of the (100) plane of NU-1000 was found in the PXRD pattern (Fig. 2). In addition, the nitrogen isotherm displayed a typical type I isotherm and does not contain a mesoporous step (Fig. 3). With a phase-pure material in hand, we sought to capitalize on the microporous nature of NU-901 for gas separation applications.

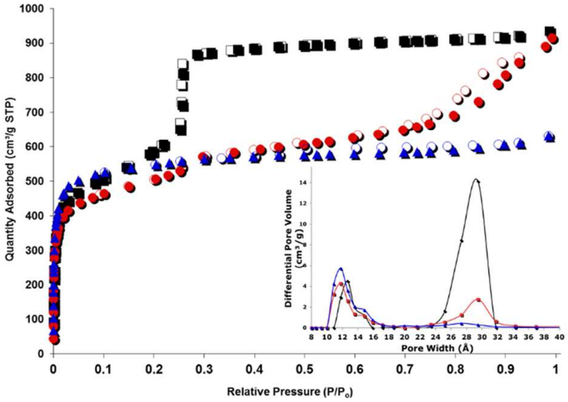

Fig. 3. Nitrogen isotherms and pore size distribution of HCl-activated MOFs synthesized with $ZrO(NO_3)_2$ + BA = NU-1000 (black squares), $Zr(acac)_4$ + BA = NU-1000/NU-901 (red circles), $Zr(acac)_4$ + 4-NH_2-BA = NU-901 (blue triangles). BA = benzoic acid. Solid

symbols = adsorption, open symbols = desorption. Inset graph is corresponding pore size distribution.

Recently, Deria et al.,[44] explored the use of SALI to incorporate perfluoroalkane groups into NU-1000 for CO_2 adsorption. A systematic increase in isosteric heats of adsorption relative to the unfunctionalized NU-1000 (Q_{st} = 24-34 kJ/mol vs 17 kJ/mol) was achieved through increasing chain lengths of perfluoroalkanes. While a proof of concept was presented by increasing pore hydrophobicity, the large mesopores of NU-1000 did not allow multiple pore wall interactions with CO_2 and therefore the uptakes achieved were only moderate as the total CO_2 adsorption at 1 bar slightly decreased (~1.8 vs 1.3 mmol/g).

Throughout the vast MOF literature there have been ample reports of functionality enhancing CO_2 adsorption. Given its amine functionality (~4 modulators per Zr_6 node), we hypothesized that NU-901-BA-NH_2 (BA = benzoic acid) would be a better system than unfunctionalized NU-1000-act (act=HCl-activated) for CO_2 adsorption. Although comprised of the same building blocks, the pore size of NU-901-BA-NH_2 is nearly one-third that of NU-1000-act (12 vs 31 ⍰ respectively, Fig. S11-12†) yet significantly outperforms its mesoporous counterpart in CO_2 adsorption (Fig. 4, Table 1). The enhanced CO_2 adsorption is attributed to the amine functionalities tethered to the SBU as corroborated by the diminished performance of HCl-activated NU-901 (Fig. 4, Table 1).

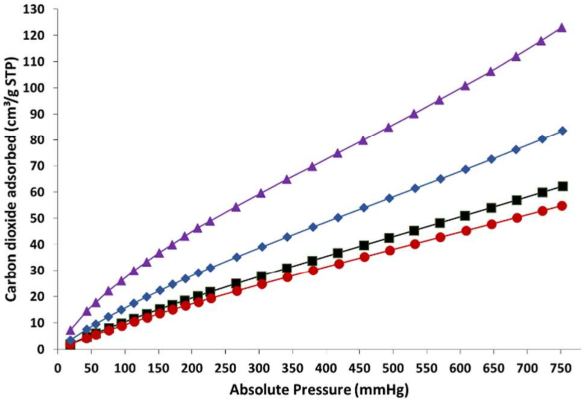

Fig. 4. CO_2 isotherms at 273K of HCl-activated NU-1000 (black squares), HCl activated NU-901 (red circles), NU-901-BA-NH_2 (blue diamonds), and NU-901-SALI-BA-3,5-NH_2 (purple triangles).

In an effort to further enhance CO_2 adsorption, we attempted to incorporate other amine moieties within NU-901. Our initial attempts focused on the use of functionalized benzoic acids as modulators during MOF synthesis. While the use of $Zr(acac)_4$ with other modulators led to the selective formation of MOFs with **scu** topology (Fig. S15, S17†), the degree of modulator incorporation depended on their acidity. For instance, the use of 4-bromobenzoic acid resulted in NU-901-BA-Br with 100% modification (~4 modulators per Zr_6 node) and 4-(methylamino)benzoic acid resulted in NU-901-BA-$NHCH_3$ with 50% modification, while the use of 4-(dimethylamino)bezoic acid led to NU-901-BA-$N(CH_3)_2$ with a lower amount (~1 per node) of modulator incorporation based on ^1H NMR (Fig. S4-S6†). Not surprisingly, based on the number and type of amine-functionalized modulators, both NU-901-BA-$NHCH_3$ and NU-901-BA-$N(CH_3)_2$ gave diminished CO_2 adsorption relative to NU-901-BA-NH_2 (Table 1, Fig. S23†.) Consequently, our efforts to functionalized NU-901 shifted to post-synthetic modification.

Table 1. Surface area, # of incorporated modulator, and CO_2 uptake of MOFs.

MOF	Surface area (m^2/g)[a]	Modulators incorporated[b]	CO_2 uptake[c]
NU-1000-act[d]	2270	0	62
NU-901-act[d]	2276	0	54
NU-901-BA-NH_2[e]	1628	4	84
NU-901-BA-$NHCH_3$[e]	2070	2	62
NU-901-BA-$N(CH_3)_2$[e]	2029	1	51
NU-901-SALI-isonic[f]	1768	3	70
NU-901-SALI-nico[f]	1770	2	84
NU-901-SALI-BA-3,5-NH_2[f]	1793	1	123

[a]BET. [b]Per node, based on ^1H NMR of disgested samples. [c]cm^3/g at ~750 mmHg, 273 K. [d]HCl activated. [e]*de novo* MOF synthesis. [f]SALI modified.

Through the use of SALI, various amine moieties could be incorporated into NU-901. However, similar to our previous *de novo* strategies, attempts to fully incorporate the relatively less acidic 4-(methylamino)benzoic acid (pKa = 5.04 vs 2.45 for 4-aminobenzoic acid)[45] through SALI resulted in only ~50% modification (Fig. S7†). We additionally explored the effect of subsitituent positioning (*meta* vs *para*) on CO_2 adsorption. Under analogous SALI reaction conditions isonictonic and nicotinic acids were incorporated into NU-901 with 75% and 50% modification respectively (Fig. S8-S9†). Although possessing a lower amount of modulators than NU-901-SALI-isonic, NU-901-SALI-nico displays enhanced CO_2 adsorption (Table 1, Fig. S24†). This difference in CO_2 affinity may be attributed to the basicities of the *para*- and *meta*-pyridine moieties (pKa = 3.73 and 4.75 respectively).[46]

We then explored the effect of multiple amine moieties within the benzoic acid modulator on the adsorption of CO_2. Given the observed enhanced CO_2 adsorption of the *meta*- positioning within nicotic acid relative to isonicotinic acid, we then attempted to modify NU-901 with 3,5-diaminobenzoic acid. Under analogous SALI reaction conditions as other prior benzoic acids, only ~25% modification was observed within NU-901-SALI-BA-3,5-NH_2 as evidenced by ^1H NMR (Fig. S10†). However, incorporation of the *meta*-diamine moieties resulted in more than double the CO_2 adsorption relative to NU-901-act (Fig. 4 Table 1). Unlike the CO_2 isotherm of NU-901-act or NU-1000-act, the isotherm of NU-901-SALI-BA-3,5-NH_2 displays a non-linear isotherm at lower pressures. The Lewis-basic amines within the MOF enhances the adsorption of the Lewis-acidic CO_2 molecules as evident in the calculated isosteric heat of adsorption (Q_{st}) of NU-901-SALI-BA-3,5-NH_2 which is greater than that of NU-901-act (25 vs 17 kJ/mol respectively Fig. S18†). We postulate that amine accessibility within the MOF contributes to this behaviour at lower pressures. Although NU-901-BA-NH_2 displays enhanced adsorption, the isotherm is more linear than that of NU-901-SALI-BA-3,5-NH_2. Utilizing computational modeling we found that the position of the 4-amino benzoic acid around the Zr_6 clusters in NU-901-BA-NH_2 significantly reduces access to the microporous channels and more importantly, encumbers access to the amino groups. As seen in Fig. S25, the amino moieties from adjacent modulators are in close proximity to one another restricting CO_2 interaction. In contrast, the pore environment within NU-901-SALI-BA-3,5-NH_2 is more accessible for CO_2 adsorption.

Conclusions

In conclusion, we demonstrate that both the zirconium salt and benzoic acid modulator affect the phase purity of Zr_6-SBU based MOFs. Using $Zr(acac)_4$ in conjunction with 4-aminobenzoic acid as a modulator during *de novo* MOF synthesis promotes the selective formation of NU-901 with **scu** topology and supresses formation of NU-1000 with **csq** topology. The acidity of a benzoic acid modulator appears to regulate their incorporation to the Zr_6-SBU under both *de novo* MOF synthesis and post-synthetic incorporation. Utilizing SALI we increased the CO_2 adsorption capacity of NU-901 by more than 130% through the incorporation of 3,5-diaminobenzoic acid. We are currently working on understanding the role of Zr-salt and modulator combinations in phase formation with other MOF systems containing functionalized tetratopic carboxylate linkers.

Conflicts of interest

There are no conflicts to declare.

Acknowledgements

O.K.F. gratefully acknowledges support from Defense Threat Reduction Agency (HDTRA1-18-1-0003) and Army Research Office-STTR (W911SR-17-C-0007). J.B.D. thanks the U.S. Army for funding via the Surface Science Initiative Program (PE 0601102A Project VR9) at the Edgewood Chemical Biological Center (ECBC). This research was performed while SJG held an NRC Research Associateship award at ECBC. This work made use of the EPIC, Keck-II, and/or SPID facilities of Northwestern University's NUANCE Center, which has received support from the Soft and Hybrid Nanotechnology Experimental (SHyNE) Resource (NSF ECCS-1542205); the MRSEC program (NSF DMR-1121262) at the Materials Research Center; the International Institute for Nanotechnology (IIN); the Keck Foundation; and the State of Illinois, through the IIN.

Notes and references

1. H. Furukawa, K. E. Cordova, M. O'Keeffe and O. M. Yaghi, *Science*, 2013, **341**, 1230444.
2. O. M. Yaghi, M. O'Keeffe, N. W. Ockwig, H. K. Chae, M. Eddaoudi and J. Kim, *Nature*, 2003, **423**, 705.
3. A. Schoedel, Z. Ji and O. M. Yaghi, *Nat. Energy*, 2016, **1**, 16034.
4. M. H. Beyzavi, C. J. Stephenson, Y. Liu, O. Karagiaridi, J. T. Hupp and O. K. Farha, *Front. Energy Res.*, 2015, **2**: 63.
5. P. Guo, D. Dutta, A. G. Wong-Foy, D. W. Gidley and A. J. Matzger, *J. Am. Chem. Soc.,* 2015, **137**, 2651-2657.
6. A. J. Howarth, Y. Liu, P. Li, Z. Li, T. C. Wang, J. T. Hupp and O. K. Farha, *Nat. Rev. Mater.*, 2016, **1**, 15018.
7. M. Rimoldi, A. J. Howarth, M. R. DeStefano, L. Lin, S. Goswami, P. Li, J. T. Hupp and O. K. Farha, *ACS Catal.*, 2017, **7**, 997-1014.
8. Y. Bai, Y. Dou, L.-H. Xie, W. Rutledge, J.-R. Li and H.-C. Zhou, *Chem. Soc. Rev.*, 2016, **45**, 2327-2367.
9. J. E. Mondloch, W. Bury, D. Fairen-Jimenez, S. Kwon, E. J. DeMarco, M. H. Weston, A. A. Sarjeant, S. T. Nguyen, P. C. Stair, R. Q. Snurr, O. K. Farha and J. T. Hupp, *J. Am. Chem. Soc.*, 2013, **135**, 10294-10297.
10. W. Morris, B. Volosskiy, S. Demir, F. Gándara, P. L. McGrier, H. Furukawa, D. Cascio, J. F. Stoddart and O. M. Yaghi, *Inorg. Chem.*, 2012, **51**, 6443-6445.
11. P. Deria, D. A. Gómez-Gualdrón, I. Hod, R. Q. Snurr, J. T. Hupp and O. K. Farha, *J. Am. Chem. Soc.*, 2016, **138**, 14449-14457.
12. M. Lammert, H. Reinsch, C. A. Murray, M. T. Wharmby, H. Terraschke and N. Stock, *Dalton Trans.*, 2016, **45**, 18822-18826.
13. D. Feng, Z.-Y. Gu, Y.-P. Chen, J. Park, Z. Wei, Y. Sun, M. Bosch, S. Yuan and H.-C. Zhou, *J. Am. Chem. Soc.*, 2014, **136**, 17714-17717.
14. T. C. Wang, W. Bury, D. A. Gómez-Gualdrón, N. A. Vermeulen, J. E. Mondloch, P. Deria, K. Zhang, P. Z. Moghadam, A. A. Sarjeant, R. Q. Snurr, J. F. Stoddart, J. T. Hupp and O. K. Farha, *J. Am. Chem. Soc.*, 2015, **137**, 3585-3591.
15. S. B. Kalidindi, S. Nayak, M. E. Briggs, S. Jansat, A. P. Katsoulidis, G. J. Miller, J. E. Warren, D. Antypov, F. Corà, B. Slater, M. R. Prestly, C. Martí-Gastaldo and M. J. Rosseinsky, *Angew. Chem. Int. Ed.,* 2015, **54**, 221-226.
16. D. Feng, W.-C. Chung, Z. Wei, Z.-Y. Gu, H.-L. Jiang, Y.-P. Chen, D. J. Darensbourg and H.-C. Zhou, *J. Am. Chem. Soc.*, 2013, **135**, 17105-17110.
17. H.-L. Jiang, D. Feng, K. Wang, Z.-Y. Gu, Z. Wei, Y.-P. Chen and H.-C. Zhou, *J. Am. Chem. Soc.*, 2013, **135**, 13934-13938.
18. T. Tanasaro, K. Adpakpang, S. Ittisanronnachai, K. Faungnawakij, T. Butburee, S. Wannapaiboon, M. Ogawa and S. Bureekaew, *Cryst. Growth Des.*, 2018, **18**, 16-21.
19. M. Taddei, *Coord. Chem. Rev.*, 2017, **343**, 1-24.
20. W.-G. Liu and D. G. Truhlar, *Chem. Mater.*, 2017, **29**, 8073-8081.
21. J. Ma, L. D. Tran and A. J. Matzger, *Cryst. Growth Des.*, 2016, **16**, 4148-4153.
22. J. Pang, S. Yuan, J. Qin, C. Liu, C. Lollar, M. Wu, D. Yuan, H.-C. Zhou and M. Hong, *J. Am. Chem. Soc.*, 2017, **139**, 16939-16945.
23. P. Müller, R. Grünker, V. Bon, M. Pfeffermann, I. Senkovska, M. S. Weiss, X. Feng and S. Kaskel, *CrystEngComm*, 2016, **18**, 8164-8171.
24. Y.-B. Zhang, H. Furukawa, N. Ko, W. Nie, H. J. Park, S. Okajima, K. E. Cordova, H. Deng, J. Kim and O. M. Yaghi, *J. Am. Chem. Soc.*, 2015, **137**, 2641-2650.
25. P. Li, Q. Chen, T. C. Wang, N. A. Vermeulen, B. L. Mehdi, A. Dohnalkova, N. D. Browning, D. Shen, R. Anderson, D. A. Gómez-Gualdrón, F. M. Cetin, J. Jagiello, A. M. Asiri, J. F. Stoddart and O. K. Farha, *Chem*, 2018, **4**, 1022-1034.
26. H. Furukawa, F. Gándara, Y.-B. Zhang, J. Jiang, W. L. Queen, M. R. Hudson and O. M. Yaghi, *J. Am. Chem. Soc.*, 2014, **136**, 4369-4381.
27. Y. Zhang, X. Zhang, J. Lyu, K.-i. Otake, X. Wang, L. R. Redfern, C. D. Malliakas, Z. Li, T. Islamoglu, B. Wang and O. K. Farha, *J. Am. Chem. Soc.*, 2018, **140**, 11179-11183.
28. F. Zhenlan, B. Bart, D. V. D. E. and F. R. A., *Angew. Chem. Int. Ed.*, 2015, **54**, 7234-7254.
29. P. Li, R. C. Klet, S.-Y. Moon, T. C. Wang, P. Deria, A. W. Peters, B. M. Klahr, H.-J. Park, S. S. Al-Juaid, J. T. Hupp and O. K. Farha, *Chem. Commun.*, 2015, **51**, 10925-10928.
30. G. C. Shearer, S. Chavan, S. Bordiga, S. Svelle, U. Olsbye and K. P. Lillerud, *Chem. Mater.*, 2016, **28**, 3749-3761.
31. H. Garcia, S. Navalon, *Metal-Organic Frameworks Applications in Separations and Catalysis*, Wiley-VCH, Weinheim, 2018.

32. G. W. Peterson, M. R. Destefano, S. J. Garibay, A. Ploskonka, M. McEntee, M. Hall, C. J. Karwacki, J. T. Hupp and O. K. Farha, *Chem. Eur. J.*, 2017, **23**, 15913-15916.
33. A. M. Bumstead, D. B. Cordes, D. M. Dawson, K. K. Chakarova, M. Y. Mihaylov, C. L. Hobday, T. Düren, K. I. Hadjiivanov, A. M. Z. Slawin, S. E. Ashbrook, R. R. R. Prasad and P. A. Wright, *Chem. Eur. J.*, 2018, **24**, 6115-6126.
34. F. Drache, V. Bon, I. Senkovska, J. Getzschmann and S. Kaskel, *Phil. Trans. R. Soc. A*, 2017, **375**.
35. V. Bon, I. Senkovska, I. A. Baburin and S. Kaskel, *Cryst. Growth Des.*, 2013, **13**, 1231-1237.
36. T. Islamoglu, K.-i. Otake, P. Li, C. T. Buru, A. W. Peters, I. Akpinar, S. J. Garibay and O. K. Farha, *CrystEngComm*, 2018.
37. T. E. Webber, W.-G. Liu, S. P. Desai, C. C. Lu, D. G. Truhlar and R. L. Penn, *ACS Appl. Mater. Interfaces*, 2017, **9**, 39342-39346.
38. S. T. Madrahimov, J. R. Gallagher, G. Zhang, Z. Meinhart, S. J. Garibay, M. Delferro, J. T. Miller, O. K. Farha, J. T. Hupp and S. T. Nguyen, *ACS Catal.*, 2015, **5**, 6713-6718.
39. Z. Li, A. W. Peters, V. Bernales, M. A. Ortuño, N. M. Schweitzer, M. R. DeStefano, L. C. Gallington, A. E. Platero-Prats, K. W. Chapman, C. J. Cramer, L. Gagliardi, J. T. Hupp and O. K. Farha, *ACS Cent. Sci.*, 2017, **3**, 31-38.
40. T. Islamoglu, S. Goswami, Z. Li, A. J. Howarth, O. K. Farha and J. T. Hupp, *Acc. Chem. Res.*, 2017, **50**, 805-813.
41. C.-W. Kung, T. C. Wang, J. E. Mondloch, D. Fairen-Jimenez, D. M. Gardner, W. Bury, J. M. Klingsporn, J. C. Barnes, R. Van Duyne, J. F. Stoddart, M. R. Wasielewski, O. K. Farha and J. T. Hupp, *Chem. Mater.*, 2013, **25**, 5012-5017.
42. M. H. Teplensky, M. Fantham, P. Li, T. C. Wang, J. P. Mehta, L. J. Young, P. Z. Moghadam, J. T. Hupp, O. K. Farha, C. F. Kaminski and D. Fairen-Jimenez, *J. Am. Chem. Soc.*, 2017, **139**, 7522-7532.
43. P. Deria, J. Yu, T. Smith and R. P. Balaraman, *J. Am. Chem. Soc.*, 2017, **139**, 5973-5983.
44. P. Deria, J. E. Mondloch, E. Tylianakis, P. Ghosh, W. Bury, R. Q. Snurr, J. T. Hupp and O. K. Farha, *J. Am. Chem. Soc.*, 2013, **135**, 16801-16804.
45. W. M. Haynes, *CRC Handbook of Chemistry and Physics, 97th Edition*, CRC Press, Boca Raton, 2016.
46. J. A. Dean, *Lange's Handbook of Chemistry, 15th Edition*, McGraw-Hill, New York, 1990.

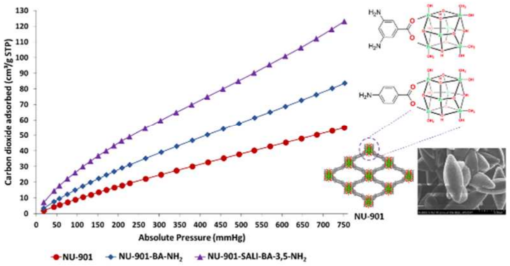

Phase-pure NU-901 was functionalized with amines through solvent-assisted linker incorporation resulting in more than double the typical CO_2 adsorption capacity.